Research Academy for Young Scientists

The Role of Dityrosine-Formation in Stabilization of Neurotoxic Amyloid-β Oligomers Associated with Alzheimer's Disease

Filip Engelhardt
engelhardtfilip@gmail.com

under the direction of
Ph.D. Nicklas Österlund
Stockholm University
Department of Materials and Environmental Chemistry

July 12, 2023

*

Abstract

Since its formulation in 1992, the amyloid cascade hypothesis, where an accumulation of amyloid-beta is thought to be a causing factor of Alzheimer's disease, has set the trajectory of Alzheimer's research. Specifically, the oligomeric amyloid-beta aggregates have been shown to be the most neurotoxic. Still, the exact mechanisms of amyloid-beta oligomers that explain why Alzheimer's disease develops remain largely unknown. To investigate these mechanisms, this study set out to examine if the neurotoxic properties of amyloid-beta oligomers can be stabilized in a membrane-like environment. Hence, amyloid-beta was prepared with LDAO to stabilize the oligomers before simulating oxidative stress by adding Copper(II) acetate and hydrogen peroxide to form covalent dityrosine bonds. The experiments then showed that dityrosine forms in oligomeric amyloid beta in a membrane-like environment and that dityrosine cross-linked oligomers might be more stable than regular amyloid-beta oligomers. Thus, this study indicates a possible cause of the development of Alzheimer's disease and where further research would be able to understand better the formed and presumably neurotoxic amyloid-beta oligomers.

Acknowledgements

I want to express my gratitude to my mentor Nicklas Österlund for his support and assistance throughout this process. I would also like to thank Rays — for excellence and their collaborative partners Beijerstiftelsen and Svenska Tekniska Vetenskapsakademien in Finland for making Rays happen. I would also like to express my gratitude to all of the Rays community, especially the students of the Rays class 2023, for showing me what a great group of people really is.

Contents

List of Abbreviations

AD Alzheimer's disease.

CD spec Circular dichrosim spectrum.

diTyr Dityrosine.

MS Mass spectrometer.

ROS Reactive oxygen species.

SEC Size Exclusion Chromatography.

ThT Thioflavin T.

Tyr Tyrosine.

1 Introduction

Alzheimer's disease (AD) is a neurodegenerative disease and type of dementia that affects the memory, speech, and behavior of affected individuals. Clinically, AD manifests through neuronal cell death and cerebral atrophy [1]. Worldwide, ∼45.0 million people are diagnosed with AD, and it is estimated to be the fifth leading cause of death globally [2]. Most AD cases are classified as sporadic, and with the expected aging of the global population, the number of people diagnosed with AD is estimated to double over the next 20 years [3]. Hence, it is also estimated that the worldwide cost of AD care will increase over the coming decades to reach a cost of 9.4 trillion US dollars by 2050, compared to approximately 2 trillion US dollars today [2].

Since the discovery of AD at the beginning of the 20th century, no one conclusion has been reached regarding the disease's molecular mechanisms. However, in 1992, Hardy and Higgins proposed that large deposition of fibrillary accumulations of amyloid-beta (Aβ) was a significant causing factor of AD [4]. Their hypothesis, the amyloid cascade hypothesis, has since established the trajectory of AD research.

1.1 Background

It was long believed that the larger aggregates of Aβ peptides and amyloid plaques played a key role in AD pathogenesis [5]. Yet, over the past decade, little improvements have been made in developing curative therapies that restore brain function in individuals with AD [5]. Instead, research has shifted toward researching smaller aggregates of Aβ, showing that smaller aggregates of Aβ are more neurotoxic than the larger amyloid aggregates and plaques [6]. Specifically, research has shown that the amyloidβ oligomers (AβO) inhabit membrane interactive properties that could cause uncontrolled leakage over the cell membrane [6]. Therefore, the amyloid cascade hypothesis has shifted toward defining (AβO) as the key contributing factor to AD mechanisms [7].

1.1.1 Amyloid-β

The Aβ peptide is a fragment formed from the larger amyloid precursor protein (APP) that forms as a result of cleavage of APP [8], when the proteases β- and γ-secretase cleave the APP, see figure 1.

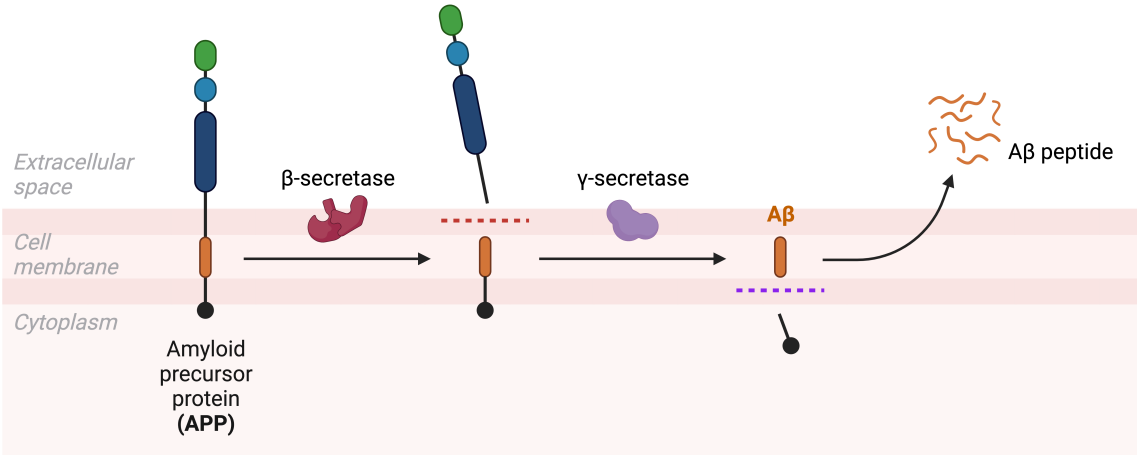

Figure 1: Amyloidogenic Pathway. Aβ formation from APP through cleavage by β- and γ-secretase in the intramembranous space [8].

The amyloid-beta fragments formed by the cleavage of APP denote peptides with an amino acid number ranging from 39 to 43. Structurally, the Aβ peptide is intrinsically disordered and forms a random coil secondary structure with a hydrophobic C-terminal part and a hydrophilic N-terminal part, see figure 2. The Aβ peptide also holds one tyrosine (Tyr) residue at amino acid 10 (Tyr10). [9]

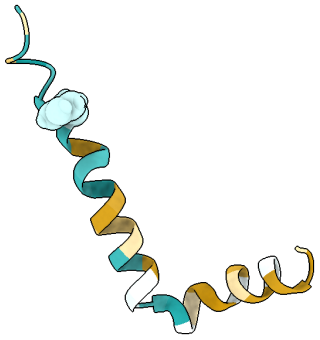

Figure 2: Structure of an Aβ-42 peptide colored according to hydrophobicity. The single Tyr residue, located within the hydrophilic segment of the peptide, is shown as a sphere [10].

Furthermore, in the human body, the Aβ-40 and Aβ-42 peptides are most prevalent

in the human body [11]. Research has shown that the Aβ-42 peptide is more prone to aggregating than Aβ-40, which implies aggregation to more neurotoxic Aβ aggregates [12]. The oligomeric aggregates have also been shown to form beta-barrel structures that interact with the cell membrane [13]. These beta barrels are pore-like structures that cause uncontrolled leakage over the cell membrane, prohibiting cells from maintaining their functional state as the concentration gradient of metal ions is depleted and homeostasis disrupted [13].

However, no causative relation between the prevalence of fibrillar Aβ aggregates in the brain and cognitive degradation has been found. Instead *in vitro* studies have indicated that oxidative stress might interact with the smaller AβO to form a more stable form of neurotoxic oligomer. This could be an indication of why the disease develops. [11]

1.1.2 Dityrosine Formation

Regular AβO are bonded together by non-covalent interactions, where the hydrophobic C-terminals of the peptides attract together, while the hydrophilic N-terminals of the peptides extend out from the hydrophobic segment of the oligomer, see figure 3.

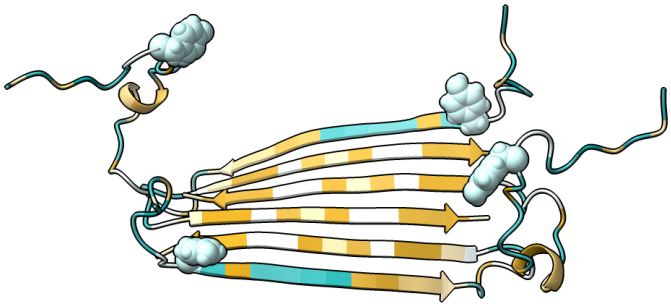

Figure 3: Structure of an Aβ-42 tetramer colored according to hydrophobicity. The Tyr residues, located within the hydrophilic segment of the peptide, are shown as spheres [10].

It is further known that metal ions like Cu, Zn, and Fe bind to the Tyr residue of the Aβ peptide to form metal ion-Tyr cross-links [14]. The binding of these metal ions to the Tyr residue can form reactive oxygen species (ROS) in proximity to the peptide, which has been shown to induce covalent dityrosine (diTyr) cross-links together with redox-active Cu or Fe ions [15]. Specifically, diTyr cross-links comprise covalent carbon between the

aromatic rings of Tyr residues, see figure 4, that stabilizes the oligomer, decreasing the propensity in which AβO aggregate into larger fibrillar structures, and thus becoming less toxic.

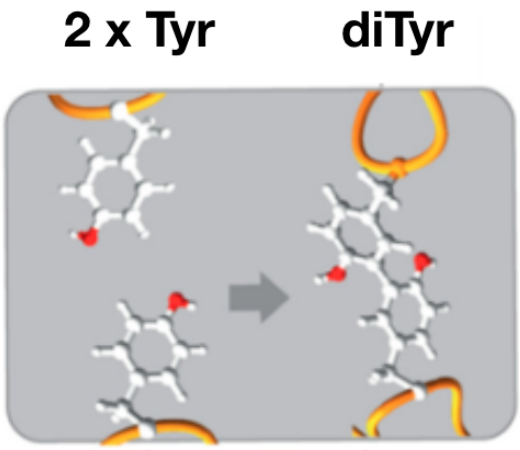

Figure 4: Dityrosine formation where Aβ binds covalently.

However, no published research has presented data about the formation and structural stabilization of diTyr cross-linked oligomers in a membrane-like environment, which could possibly be a cause of the stabilization of neurotoxic oligomeric pore structures. Furthermore, it is not known if the Tyr residues are available to interact with redox-active ions to form diTyr cross-links. Additionally, it has not published any data on whether the chemically explained stabilization of AβO is consistent with oligomers in membranous environments.

1.1.3 Bio-Membranes

Bio-membrane mimics comprise surfactant monomers that form micelles, which are compounds made to resemble the mechanisms of biological cell membranes in *in vitro* experiments, see figure 5. Regarding evaluating the properties of the smaller aggregates of Aβ, two detergents have been found to stabilize monomeric and oligomeric states. Firstly, SDS has been found to stabilize monomers in a solution of Aβ peptides, a desired property of a detergent suited for the experiments performed in this study [16]. Secondly, LDAO was also used as a detergent for the experimental studies because it has been shown to stabilize oligomers in a solution of Aβ. LDAO is also a zwitterionic detergent, which would

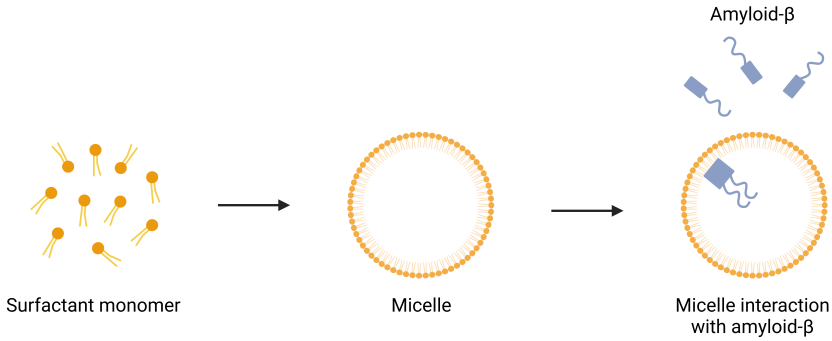

Figure 5: Micelle formation from surfactant monomers to micelles. The amphiphilic properties of the micelle then mimic the cell membrane in interacting with cellular compounds, in this regard, the Aβ peptide.

provide a well-designed membrane mimic of the human neuron [16].

Furthermore, as presented by previous research, an advantageous concentration ratio to form oligomeric structures between peptide and micelle concentration is 2:1. To calculate the desired micelle concentration, the formula

$$C_{\text{micelle}} = \frac{C_{\text{detergent}} - CMC}{N}, \tag{1}$$

where the critical micelle concentration (CMC) represents a detergent-specific value for when surfactant monomers form micelles, and N represents the number of surfactant monomers that form one micelle, was used.

1.2 Previous Research

Previously published research has addressed and observed the neurotoxicity of the oligomeric aggregates of Aβ [17]. It has also been shown that AβO can be stabilized in a membranous environment [16]. However, published research indicates no direct relationship between the accumulation of Aβ aggregates and cognitive degradation as manifested in AD [11]. Hence, it can be thought that additional factors are important to explain the stabilization of neurotoxic oligomers and, thus, disease development, compared with spontaneously aggregated Aβ.

A previous study showed that oxidative stress on Aβ peptides in a non-membrane environment might cause the formation of diTyr [14]. Therefore, this potentially stabilizing diTyr formation of Aβ might provide valuable insight into the stabilization of neurotoxicity in the brain if tested on oligomers in a membrane-like environment [15]. Therefore, it is relevant, for the understanding of the precipitating mechanism of AD, to examine further if diTyr forms in a membranous environment, in what structural way diTyr forms, and if the diTyr cross-linked Aβ is more stable than that of regular Aβ aggregates.

1.3 Aim of Study

The aim of this study was to investigate the formation and role of diTyr in neurotoxic (AβO)O connected with AD, to understand the mechanisms and causes of AD better. This was done by investigating if neurotoxic AβO are stabilized in a membrane-like environment, form diTyr cross-links, and if the formed diTyr cross-links make AβO more chemically stable than AβO without diTyr.

2 Method

In this study, methods were used to collect Aβ monomer samples, stabilize AβO, create dityrosine cross-links, and evaluate the stabilization of dityrosine cross-links.

2.1 Preparation of Monomer Sample

Aβ monomer samples from freeze-dried Amyloid-β-42 peptides (*rPeptides*). To prepare the monomer samples, the peptides were dissolved in 6 M GuHCL to make a peptide concentration of 1–1.4 mg/mL (Sigma-Aldrich, USA). Using size exclusion chromatography (SEC), with a 500 µL injection loop and a Superdex 75 Increase 10/300 GL column, fractions of 250 µL were collected at around 14 mL, where the monomer peak was detected [Product reference here. Alt. previous study research]. In the SEC column, the injected sample was eluded with TRIS buffer 1, filtered, and degassed (VWR International, China). Using a nanophotometer at an excitation wavelength of 280 nm, the concentration of the

collected monomer samples was determined. The samples with the highest concentration were then pooled together with a combined concentration ranging from 30–60 mM.

Furthermore, to stabilize monomers in a membrane-like environment as reference data, SDS was added to a 500 µL monomer sample to make an SDS sample concentration of 20 mM (Sigma-Aldrich, Japan). The sample was then run through SEC using a Superdex 75 increase 10/300 GL column to measure and detect the monomer peak.

2.2 Stabilizing Oligomers

To evaluate Aβ aggregation over time, Aβ monomeric samples were prepared with a 1:1, 1:2, and 1:3 peptide-micelle concentration ratio using a 0.5 M LDAO solution (Sigma-Aldrich, Switzerland). Thioflavin T (ThT) fluorescence was then added to make a sample concentration of 40 µM ThT. Subsequently, the fluorescence spectrophotometer was run for 24 h at 25 °C [find ref] and fluorescence intensity was measured every 15 min at a wavelength of 482 nm.

The formation of AβO was also monitored through circular dichroism spectrophotometry (CD spec), which measured the secondary structure of the peptide samples, and size exclusion chromatography (SEC). One 500 µL monomeric sample was prepared with 0.5 M LDAO to have a peptide-micelle ratio of 2:1. Another 500 µL monomer sample was prepared without the LDAO detergent and incubated for 16 h at 25 °C. To examine the secondary structure over time of the sample with LDAO, the sample was incubated in the CD spectrometer and incubated in the CD spectrophotometer for 16 h. Measurements of the secondary structure were taken every 10 min. Subsequently, 200 µL of the monomeric samples, with and without detergent, both incubated at 25 °C for 16 h, were run through an SEC. The SEC was performed separately on both samples using a Superdex 75 Increase 10/300 GL column. The sample without added detergent was eluded with TRIS buffer 1, and the sample with added LDAO was eluted with TRIS buffer 2 1. A sample volume of 500 µL was used to perform the SEC on both samples.

Additionally, a monomeric sample with LDAO was prepared. 100 µL of the sample was then run through SEC without incubation. The SEC was performed using a Superdex 200

Table 1: Prepared buffers

Buffers	Contents
TRIS buffer 1	20 mM TRIS-HCL at pH 9, 100 mM NaCl
TRIS buffer 2	20 mM TRIS-HCL at pH 9, 100 mM NaCl, 3.4 mM LDAO
TRIS buffer 3	20 mM TRIS-HCL at pH 9, 100 mM NaCl, 10 mM LDAO
TRIS buffer 4	20 mM TRIS-HCL at pH 9, 100 mM NaCl, 20 mM SDS

increase 5/150 GL column and the sample was eluted with TRIS buffer 2. Subsequently, SEC was performed on a 100 mL monomer sample without LDAO, using TRIS buffer 1 and a Superdex 200 increase 5/150 GL column.

The stability of AβO was further examined by varying the concentrations of LDAO detergent, and by using SDS detergent. A 200 µL monomer sample was prepared with an LDAO concentration of 10 mM and, eluded with TRIS buffer 3, the sample was run through the SEC using a Superdex 200 increase 5/150 GL column. Additionally, another SEC was performed on a 200 µL monomer sample with a detergent concentration of 20 mM SDS. The sample was eluded with TRIS buffer 4 to investigate potential changes in the composition of the Aβ-peptides compared with the LDAO detergent.

Furthermore, to evaluate the secondary structures of the peptide sample with a detergent concentration of 10 mM LDAO, 200 µL of the sample was run on the CD spec for 15 h with measurements taken every 15 min.

2.2.1 Oligomer Aggregate Composition

The composition and size of the Aβ aggregates in an LDAO solution with and without diTyr cross-links were detected using a mass spectrometer (MS). To prepare the samples, 1 mg of freeze dried peptide was dissolved in 0.7 µL ammonium acetate (200 mM at pH 9) (Sigma-Aldrich, USA). An MS capillary was then filled with 5 µL of the prepared sample with an LDAO concentration of 3.4 mM and an ammonium acetate concentration of 200 mM. The sample was then sprayed through the MS at a collision energy of 20 eV. Subsequently, an MS capillary was filled with 5 µL of the diTyr cross-linked sample, with an LDAO concentration of 3.4 mM, and an ammonium acetate concentration of 200 mM. Subsequently, the sample was sprayed through the ms with a collision energy of 20 eV.

2.3 Dityrosine Cross-Linking

Three 400 µL monomeric samples were prepared with a 50 µM peptide concentration. 0.5 M LDAO was added to one of the samples to make a detergent concentration of 3.4 mM LDAO. The second sample was prepared to have a 20 mM SDS and the third sample was prepared without detergent.

Subsequently, the binding of copper ions to Aβ was evaluated by measuring the quenching of Tyr10 fluorescence upon the addition of Cu^{2+}. Tyr signals were detected using an excitation wavelength of 260 nm and an emission wavelength of 305 nm. 1 µM. 1 mM Cu(II) acetate monohydrate was added to the samples, and measurements were taken every 1 µL of added Cu(II) acetate monohydrate until a final sample concentration of 25 µM was reached (Fuka, Germany).

The three sample conditions, without detergent, with 3.4 mM LDAO, and with 20 mM SDS, were then placed in the fluorescence spectrophotometer, where both Tyr and diTyr signals were detected over 2 h for respective sample. The Tyr signal was measured using an excitation wavelength of 260 nm and an emission wavelength of 305 nm and the diTyr signal was measured using an excitation wavelength of 320 nm and an emission wavelength of 405 nm. To initiate the diTyr cross-linking, a 7.5 M H_2O_2 solution was added to make a sample concentration of 250 µM H_2O_2 (Sigma-Aldrich). Subsequently, the secondary structure of the samples was measured with CD spectroscopy before and after diTyr cross-linking, using a 1 mm cuvette and 200 µL of the sample.

2.3.1 Evaluating the Composition of Cross-Linked AβO

To evaluate the composition of AβO, 500 µL of monomer sample with a detergent concentration of 3.4 mM LDAO was prepared and cross-linked with diTyr, using a 2 mM Cu(II) acetate monohydrate soultion and a 7.5 M H_2O_2 solution to make a sample concentration of 25 µM Cu(II) acetate monohydrate and 250 µM.

After incubating at room temperature for 2 hour, the cross-linked sample was run through SEC using a Superdex 75 increase 10/300 GL column. The samples were eluded with TRIS buffer 2. The detected peaks were fractioned and collected. Subsequently, the

peptide concentration of the sample was determined by using a nanophotometer with an excited wavelength of 280 nm. A fluorescence spectrophotometer was then used to measure the diTyr signals of each fraction. The excitet wavelength was 320 nm and the emitted wavelength was 405 nm. After detecting diTyr fluorescence, the samples were measured for their secondary structure using CD spec.

Subsequently, the monomer samples were prepared with an LDAO concentration of 3.4 mM, using a 0.5 M LDAO solution. One sample was then cross-linked with diTyr using a 2 mM Cu(II) acetate monohydrate soultion and a 7.5 M H_2O_2 solution to make a sample concentration of 25 µM Cu(II) acetate monohydrate and 250 µM. The sample was then incubated at room temperature for 2 h. An MS was then used to determine the difference in mass between the Aβ samples with and without diTyr cross-links to observe the formation of diTyr. Furthermore, the MS was used to, in an extended manner, observe the composition and mass of the cross-linked Aβ aggregates.

2.4 Analyzing Dityrosine Stabilization

To evaluate the stability of diTyr cross-links, four monomer samples were prepared under different conditions. One sample was made to have an SDS concentration of 20 mM SDS. Two samples were prepared to have an LDAO concentration of 3.4 mM LDAO where one sample was diTyr cross-linked. Another monomer sample was used as a control. 30 µL of each sample was pipetted into Eppendorf tubes, before adding 10 µL of Laemmle sample buffer to each tube (Bio-Rad Laboratories, Inc, USA). Two SDS polyacrylamide gels were prepared by pipetting 20 µL from each eppendorf tube onto separate wells of the gel of each gel (Bio-Rad Laboratories, Inc, USA). 5 µL of protein ladder was added on both sides of the samples in both gels. Subsequently, the gel was run for 30 min at 200 V in SDS running buffer. After running the gels, one gel was colored overnight before then being decolored. The other gel was developed using the Thermo-scientific silver staining protocol (Thermo Scientific).

3 Results

3.1 Amyloid-β Oligomer Formation

Figure 6 shows the ThT intensity of fibrillar Aβ aggregates. Compared to the sample without detergent, which is found in theory to aggregate into larger fibrils over time, it can be seen how the sample with added LDAO is stabilized at a fluorescent intensity approximately five times lower than that of the sample without LDAO.

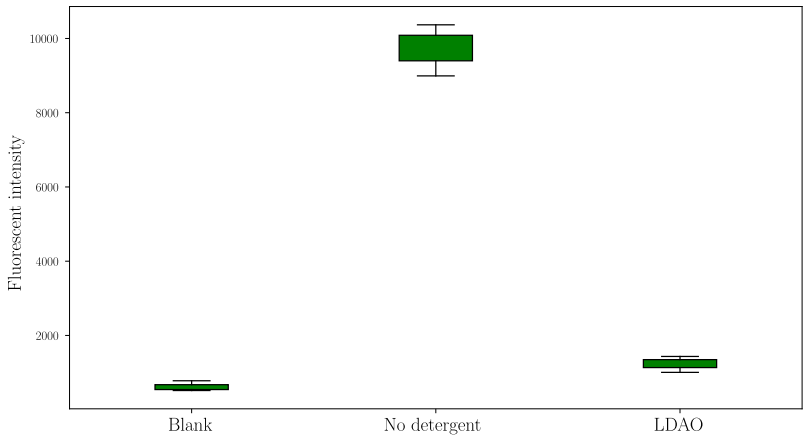

Figure 6: Average of fluorescence intensity over 24 h with a blank sample with TRIS buffer 2, a sample without detergent, and a sample with a detergent concentration of 3.4 mM. Error bars represent the value range recorded.

Furthermore, Figure 7 shows SEC chromatograms of a monomeric sample, before and after incubation, and a sample with 3.4 mM LDAO after incubation. The graphs illustrate a shift in size between the samples, where, after incubating the sample without detergent, aggregates to larger aggregates that are collected in the void around 8 mL. After incubating the sample with added LDAO, it can be seen how it has aggregated into smaller aggregates that are fractioned around 10 mL.

Figure 8 shows the secondary structures of the samples run through the SEC. The graph demonstrates a shift in secondary structures from a random coil in the monomer sample without detergent to the incubated samples. In both samples incubated for 16h, the CD spec measured beta-structures.

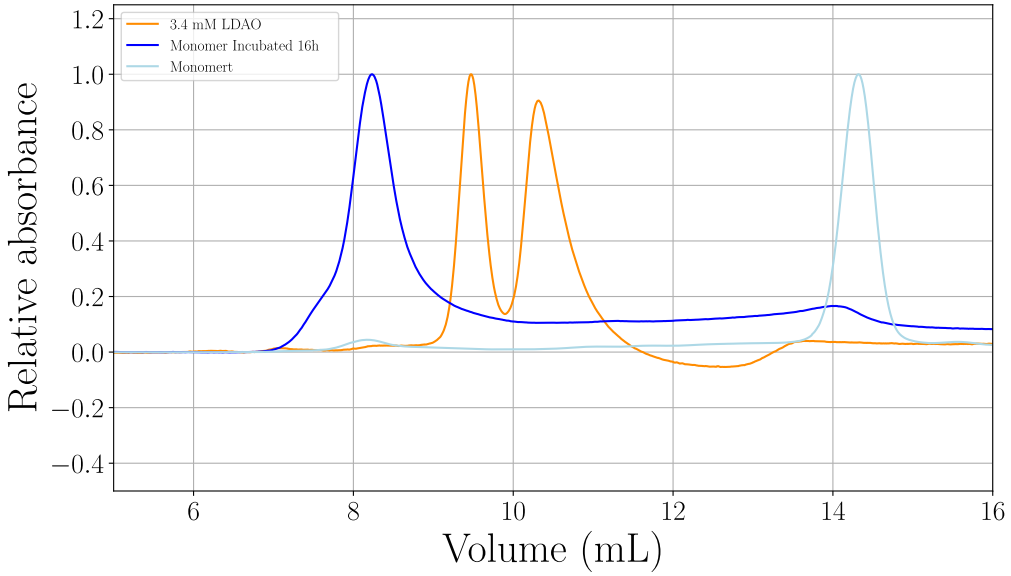

Figure 7: Normalized SEC data of Aβ samples showing size fractions, represented by volume run through the SEC column. At the void volume of 8 mL, segments with a greater mass than 70 000 kDa are shown in the graph.

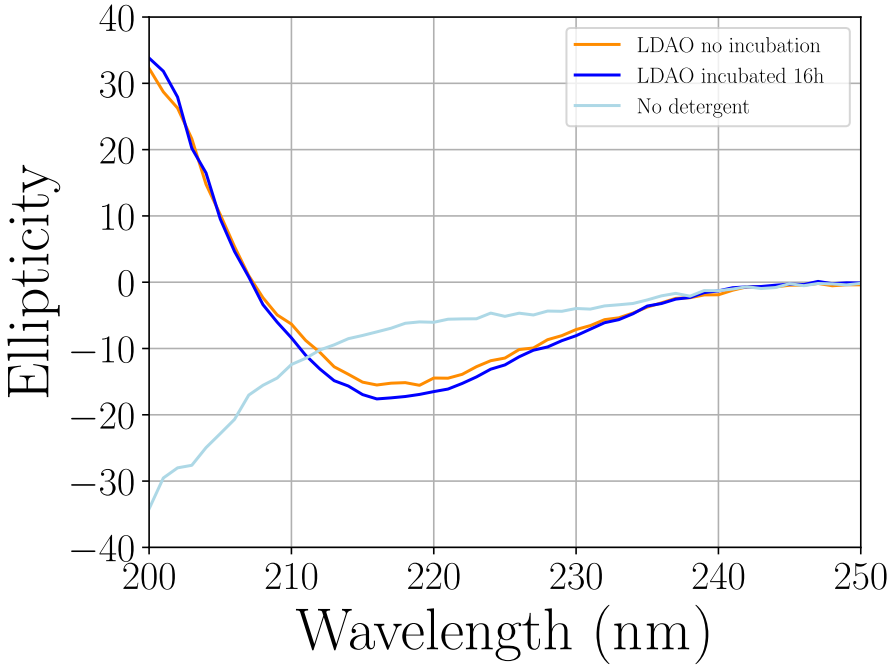

Figure 8: Secondary structures of Aβ samples.

3.2 Dityrosine Assay

Figure 9 shows the change in tyrosine fluorescence intensity at different sample concentrations of copper. In both samples, it can be seen that the addition of copper to the sample quenches the tyrosine fluorescence signal, but where the sample without LDAO experienced a larger decrease in the Tyr signal.

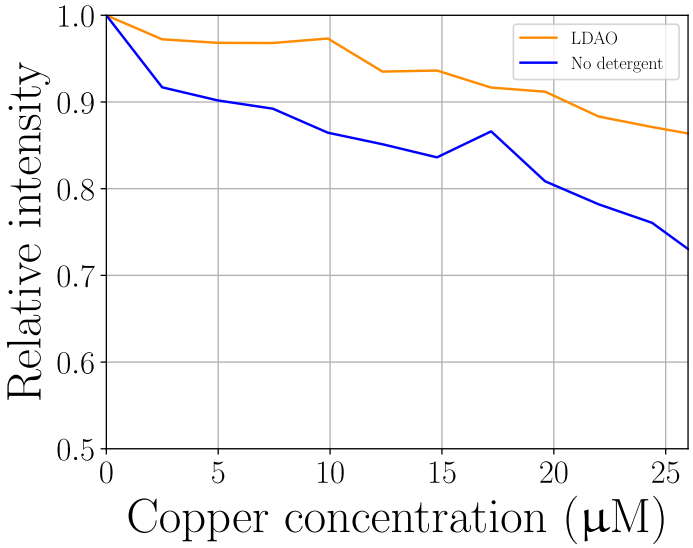

Figure 9: Fluorescence intensity in relation to the copper concentration. Fluorescence was measured with an excitation wavelength of 260 nm and an emission wavelength of 305 nm.

Figure 10, shows a change in tyrosine and diTyr fluorescence signals over time in samples without detergent, with LDAO, and with SDS. Graphed, over time, figure 10 shows an increase in the diTyr signal and a decrease in the diTyr signal in all samples.

Figure 11 shows a comparison between SEC and CD performed on monomer samples with LDAO before and after diTyr cross-linking. Figure 11a shows SEC data of LDAO samples. As can be seen in the sample with diTyr cross-link, the prevalence of smaller aggregates increased compared with before cross-linking the sample. Figure 11b shows the secondary structure of the LDAO samples, demonstrating beta structure in both samples.

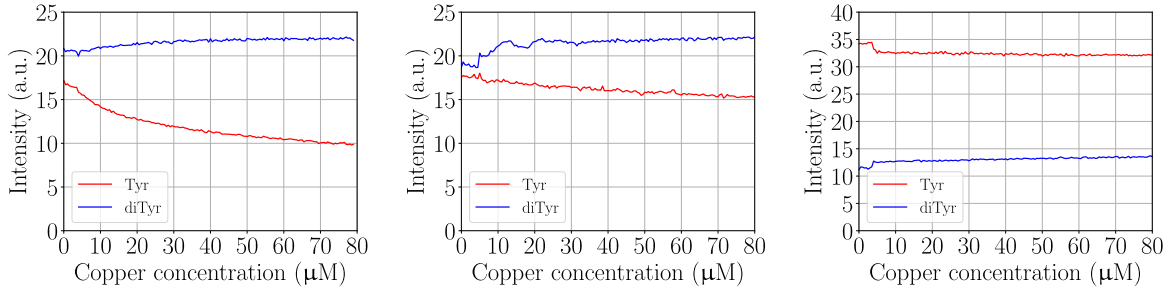

(a) No detergent (b) LDAO (c) SDS

Figure 10: Fluorescence showing tyrosine and diTyrosine intensity. Tyrosine was measured using an excitation wavelength of 260 nm and an emission wavelength of 305 nm. DiTyrosine was measured with an excitation wavelength of 320 nm and an emission wavelength of 405 nm. Please also note that the x-axis shows a fluorescent signal over time and not copper concentration.

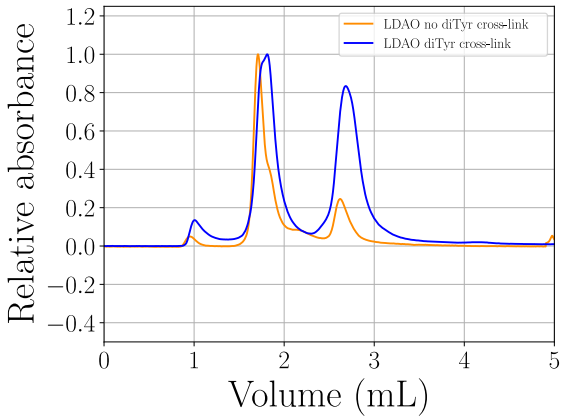

(a) Comparison between size fractions from LDAO samples before and after diTyr cross-link.

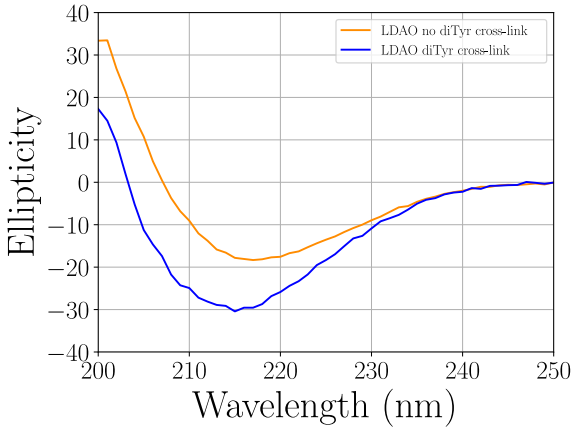

(b) Secondary structure of LDAO samples before and after diTyr cross-link.

Figure 11: Illustration of LDAO size fractions with and without diTyr cross-links compared with the recorded secondary structure of both size fractions. For more comparisons of diTyr formation in different detergents and detergent concentrations, see Appendix A.

Shown in figure 12 is a mass spectrogram of an LDAO sample without diTyr cross-links. The depicted bars show compound mass over the number of charges, which could be aggregates of the size of oligomers. See Appendix B for a table of the possible exact masses.

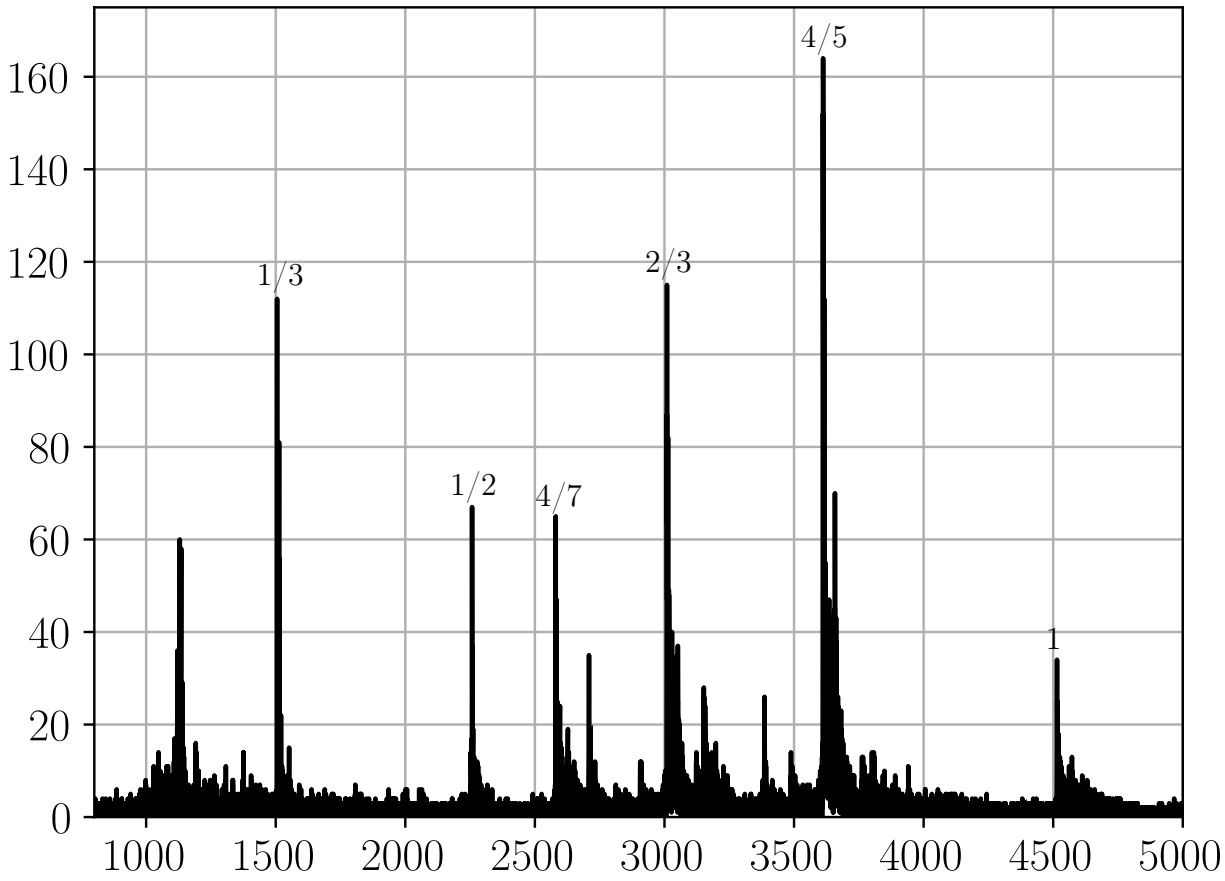

Figure 12: Mass spectrometry of sample without diTyr-cross-links performed at a collision energy of 20 V. The marks above the bars indicate the simplified ratio of oligomer number over the number of charges.

Shown in figure 13 is a mass spectrogram of an LDAO sample without diTyr cross-links. The depicted bars show compound mass over the number of charges, which shows the presence of aggregates that could be the size of oligomers. See Appendix B for a table of the possible exact masses.

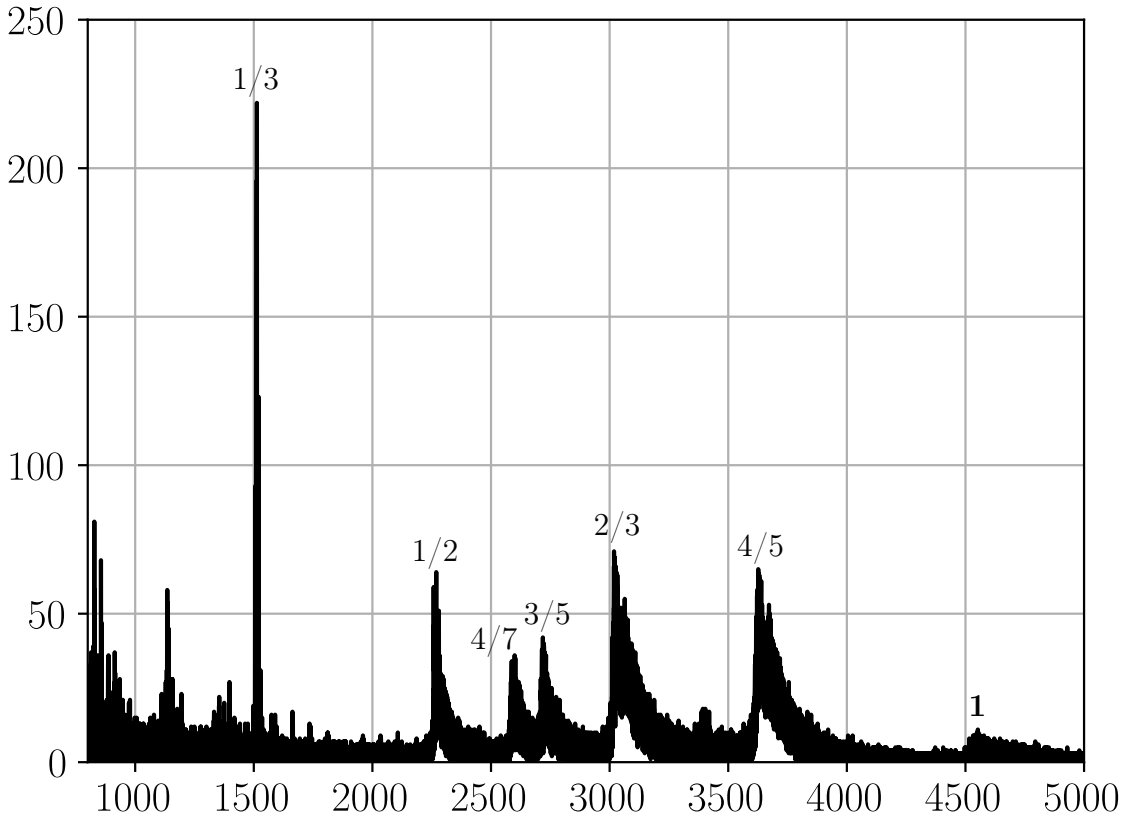

Figure 13: Mass spectrometry of sample with diTyr-cross-links performed at a collision energy of 20 V.The marks above the bars indicate the simplified ratio of oligomer number over the number of charges.

Furthermore, figure 14 shows the different secondary structures of the fractions collected from an oligomeric sample with diTyr cross-links. The CD spec measurements from the different fractions show a minimum at around 218 nm, which indicates a beta structure of the compounds in the sample.

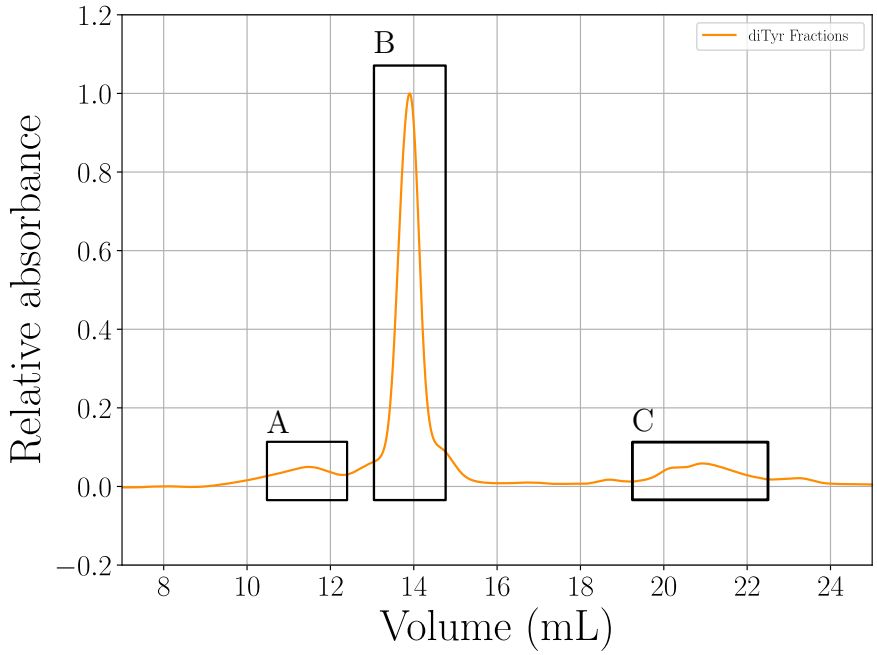

(a) SEC of an oligomeric sample with diTyr cross-links. The fractions A-C were collected around the peaks of the respective fractions.

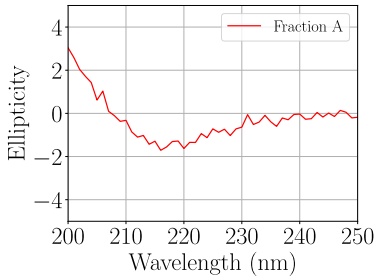

(b) CD spec performed in fraction A.

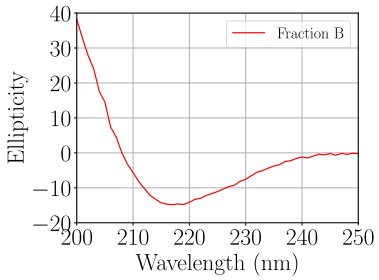

(c) CD spec performed in fraction B.

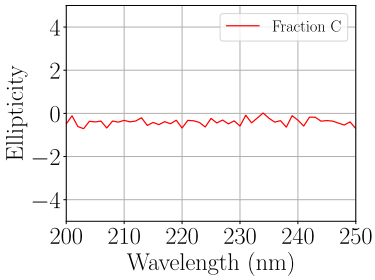

(d) CD spec performed in fraction C.

Figure 14: Fractions collected from an oligomeric sample with diTyr compared with CD spec on respective fraction. The CD spec recorded the excited wavelength from 300–350 nm.

It can be seen in figure 15 the measured fluorescent intensities at different wavelengths. All samples show a maximum at around 360 nm, but fraction B can be seen to emit relatively higher intensities of light at wavelengths up to around 420 nm.

As can be seen in figure 16, the diTyr cross-liked sample with LDAO detergent does not show the smaller aggregates that the sample without diTyr and the sample with diTyr cross-links in the SDS solution show. However, all three samples lines around the 20 kDa

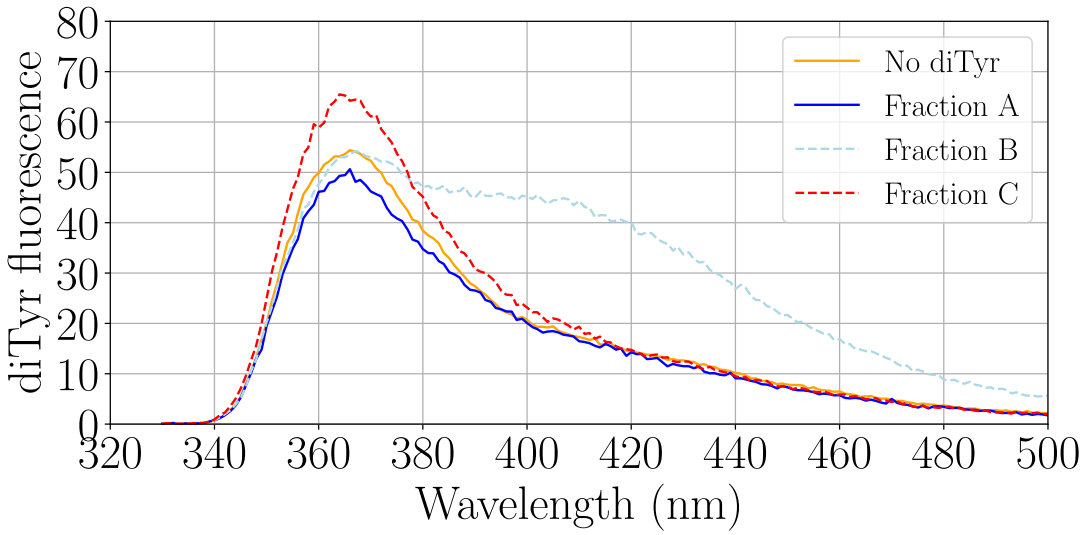

Figure 15: Fluorescent spectrum. The fluorescence was measured with an exciting wavelength of 320 nm at wavelengths ranging from 320–500 nm

.

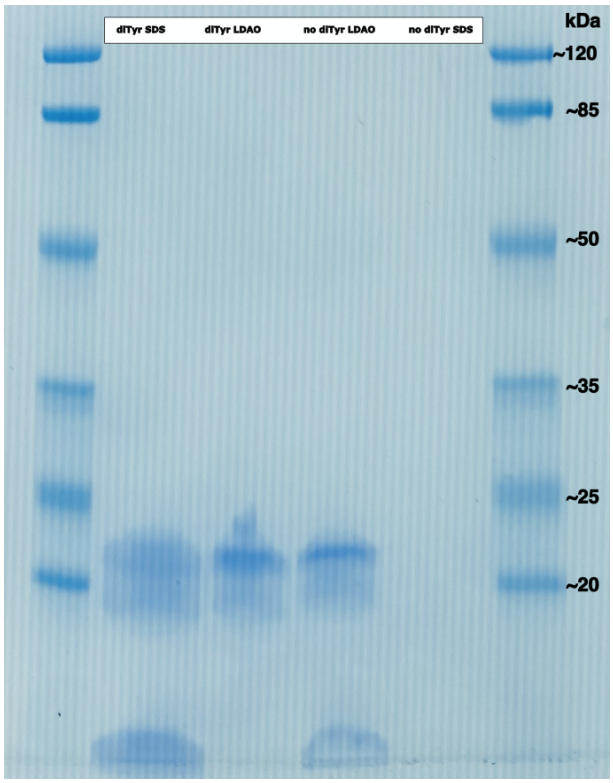

Figure 16: SDS polyacrylamide gel electrophoresis. Pierce™ Prestained Protein MW Marker was used as a color ladder.

4 Discussion

This study shows how the N-terminal and Tyr residues of AβO in a membranous environment are available to interact with metal ions and form covalent diTyr. The study also presents supporting evidence that the formation of diTyr occurs in the AβO in membranous environments. Experiments also indicate the possibility that the diTyr cross-linked AβO are more stable than Aβ without diTyr cross-links. Still, due to a low number of experiments performed to determine the stabilization, no statistically significant conclusions can be drawn in that regard.

4.1 Dityrosine Assay

Illustrated by figure 6 and figure 7, Aβ samples do not aggregate to large fibrillar Aβ aggregates if added with LDAO detergent, compared with a sample without added LDAO. Although figure 8 indicates a transition in secondary structure from random coil to beta structure, which is indicative of both oligomers and larger Aβ aggregates, the SEC curve in figure 7 shows that the sample with added LDAO detergent contains smaller aggregates than in the sample without added LDAO. The difference in size over time also confirms previous data on AβO stabilization in LDAO detergent.

As shown in figure 9, copper ions quench the tyr signal in an LDAO sample. This indicates that the hydrophilic N-terminals and tyr residues are available to interact in AβO in a membranous environment. As shown in figure 10, the copper quenching also occurs similarly to the sample with SDS detergent and the control sample previously shown to interact with copper. Furthermore, figure 10 also indicates the formation of diTyr, due to an increase in diTyr signal, in the sample without detergent, with LDAO, and with SDS, indicated by the rise in diTyr fluorescent signal. Thus, this study shows that diTyr forms in an Aβ sample with LDAO.

Additionally, the three fractions collected from a diTyr cross-linked sample with added LDAO, seen in figure 14, provide results that demonstrate how the diTyr formation occurs in AβO. First, fraction B, collected from SEC, showed a beta structure indicative of an aggregated form of Aβ. Second, as shown in figure 14, fraction B expressed diTyr signals

on the tyr fluorescence spectrometry. Combined with the compound mass noted by the SEC, see figure 10, and the size derived from the mass spectrometry of the diTyr sample, see figure 3, it is further shown how the diTyr cross-links occur in the AβO.

Returning to figure 19, it is reasonable to believe that the peptide concentrations were too low in fractions A and C to show accurate results because of the low intensities measured on the CD spec. However, because of the stronger signal shown in fraction B and the clear readings from both the SEC and CDS, see figure 10, for the purpose of this study, the collected data still indicate that AβO can experience diTyr cross-linking in membranous mimic.

Furthermore, as shown in figure 16, the SDS gel shows no separation of the oligomer compounds in the diTyr cross-linked sample with LDAO compared with the LDAO sample that was not cross-linked. This indicates that the formed diTyr in the AβO might make the oligomer more stable compared to AβO without cross-linked diTyr.

4.2 Further Studies

It would be of interest to perform diTyr cross-linking experiments on Aβ in cell cultures, or *in vivo*. This would deepen the understanding of AβO interactions in a cell environment and give relevant information on the presumed stabilization of neurotoxicity in an environment where AD occurs.

Apart from performing experiments on cell cultures or *in vivo*, further research could be conducted *in vitro* with biomembrane mimic to examine additional properties of AβO. This could further support the stable diTyr cross-linked AβO hypothesis presented in this study. For example, studies could be done to evaluate the pore structure of the diTyr cross-linked AβO and monitor its specific neurotoxic properties. It would also be interesting to examine the possibility for Zn^{2+} to inhibit the membrane leakage caused by the oligomeric pores [18]. A study of such sort could thus provide additional understanding of the stabilization of diTyr cross-linked AβO and its role in stabilizing a neurotoxic state in the brain.

As can be seen in this study, Aβ interacts differently with different membrane mimics.

One explanation could be that the detergents used in this study are chemically different, where SDS is anionic and LDAO zwitterionic. However, the noticed difference in Aβ interactions with SDS and LDAO proposes how variations in the membrane structures of neurons might be more resilient to neurotoxic diTyr cross-linked AβO formation. Alternatively, different membrane compositions might result in diTyr forming in less neurotoxic Aβ aggregates or a generally decreased or increased diTyr cross-linking overall. This becomes interesting when addressing previous research on genetic membrane protein factors like the APOe4 gene, which has been shown to entail a statistically higher risk of developing AD.

4.3 Conclusion

In conclusion, this study presents data that adds to the understanding of peptide interactions connected to mechanisms that potentially could stabilize a neurotoxic state in the brain and thus cause disease. Specifically, it is shown in this study how diTyr cross-links occur in AβO in a zwitterionic environment. The results also suggest, in conjunction with the theoretical background, that the demonstrated formation of diTyr in oligomers might result in a more stable peptide than that of the regular AβO. This further indicates the possibility that diTyr cross-linking of neurotoxic AβO in a zwitterionic environment might be a causing factor of the type of neuronal cell death associated with the pathogenesis of AD, which further research would be able to explore in more detail.

References

[1] K. It and W. D. W. KNOW, "What is alzheimer's disease?," *N Engl] Med*, vol. 314, pp. 964–973, 1986.

[2] M. J. Prince, A. Wimo, M. M. Guerchet, G. C. Ali, Y.-T. Wu, and M. Prina, *World Alzheimer Report 2015 - The Global Impact of Dementia: An analysis of prevalence, incidence, cost and trends.* London: Alzheimer's Disease International, 2015.

[3] M. Prince, M. Knapp, M. Guerchet, P. McCrone, M. Prina, M. Comas-Herrera, R. Adelaja, B. Hu, B. King, D. Rehill, *et al.*, "Dementia uk: update," 2014.

[4] J. A. Hardy and G. A. Higgins, "Alzheimer's disease: the amyloid cascade hypothesis," *Science*, vol. 256, no. 5054, pp. 184–185, 1992.

[5] R. Ricciarelli and E. Fedele, "The amyloid cascade hypothesis in alzheimer's disease: It's time to change our mind," *Current Neuropharmacology*, vol. 15, no. 6, pp. 926–935, 2017.

[6] L. Mucke and D. J. Selkoe, "Neurotoxicity of amyloid β-protein: Synaptic and network dysfunction," *Cold Spring Harbor Perspectives in Medicine*, vol. 2, no. 6, p. a006338, 2012.

[7] N. Österlund, R. Moons, L. L. Ilag, F. Sobott, and A. Gräslund, "Native ion mobility-mass spectrometry reveals the formation of β-barrel shaped amyloid-β hexamers in a membrane-mimicking environment," *Journal of the American Chemical Society*, vol. 141, no. 26, pp. 10440–10450, 2019.

[8] H. Hampel, J. Hardy, K. Blennow, and et al., "The amyloid-β pathway in alzheimer's disease," *Molecular Psychiatry*, vol. 26, pp. 5481–5503, 2021.

[9] O. Crescenzi, S. Tomaselli, R. Guerrini, S. Salvadori, A. M. D'Ursi, P. A. Temussi, and D. Picone, "Solution structure of the alzheimer amyloid β-peptide (1–42) in an apolar microenvironment: Similarity with a virus fusion domain," *European journal of biochemistry*, vol. 269, no. 22, pp. 5642–5648, 2002.

[10] S. Ciudad, E. Puig, T. Botzanowski, M. Meigooni, A. S. Arango, J. Do, M. Mayzel, M. Bayoumi, S. Chaignepain, G. Maglia, S. Cianferani, V. Orekhov, E. Tajkhorshid, B. Bardiaux, and N. Carulla, "A beta (1-42) tetramer and octamer structures reveal edge conductivity pores as a mechanism for membrane damage," *Nature Communications*, vol. 11, p. 3014, 2020.

[11] M. P. Murphy and H. r. LeVine, "Alzheimer's disease and the amyloid-beta peptide," *Journal of Alzheimer's Disease*, vol. 19, no. 1, pp. 311–323, 2010.

[12] A. M. Klein, N. W. Kowall, and R. J. Ferrante, "Neurotoxicity and oxidative damage of beta amyloid 1-42 versus beta amyloid 1-40 in the mouse cerebral cortex.," *Annals of the New York Academy of Sciences*, vol. 893, pp. 314–320, 1999.

[13] D. C. Bode, M. D. Baker, and J. H. Viles, "Ion channel formation by amyloid-β42 oligomers but not amyloid-β40 in cellular membranes," *Journal of Biological Chemistry*, vol. 292, no. 4, pp. 1404–1413, 2017.

[14] C. S. Atwood, G. Perry, H. Zeng, Y. Kato, W. D. Jones, K.-Q. Ling, X. Huang, R. D. Moir, D. Wang, L. M. Sayre, *et al.*, "Copper mediates dityrosine cross-linking of alzheimer's amyloid-β," *Biochemistry*, vol. 43, no. 2, pp. 560–568, 2004.

[15] S. K. Wärmländer, N. Österlund, C. Wallin, *et al.*, "Metal binding to the amyloid-β peptides in the presence of biomembranes: Potential mechanisms of cell toxicity," *Journal of Biological Inorganic Chemistry*, vol. 24, no. 7, pp. 1189–1196, 2019.

[16] M. Serra-Batiste, M. Ninot-Pedrosa, M. Bayoumi, M. Gairí, G. Maglia, and N. Carulla, "Aβ42 assembles into specific β-barrel pore-forming oligomers in membrane-mimicking environments," *Proceedings of the National Academy of Sciences*, vol. 113, no. 39, pp. 10866–10871, 2016.

[17] A. M. Klein, N. W. Kowall, and R. J. Ferrante, "Neurotoxicity and oxidative damage of beta amyloid 1-42 versus beta amyloid 1-40 in the mouse cerebral cortex.," *Annals of the New York Academy of Sciences*, vol. 893, pp. 314–320, 1999.

[18] M. Kawahara, N. Arispe, Y. Kuroda, and E. Rojas, "Alzheimer's disease amyloid beta-protein forms zn (2+)-sensitive, cation-selective channels across excised membrane patches from hypothalamic neurons," *Biophysical journal*, vol. 73, no. 1, pp. 67–75, 1997.

A Dityrosine Formation in Different Solutions

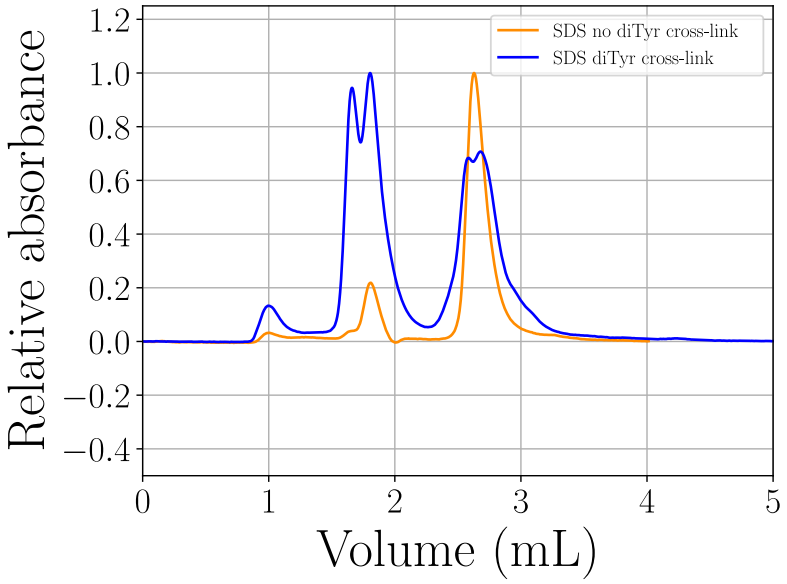

(a) Comparison between size fractions from SDS samples before and after diTyr cross-link.

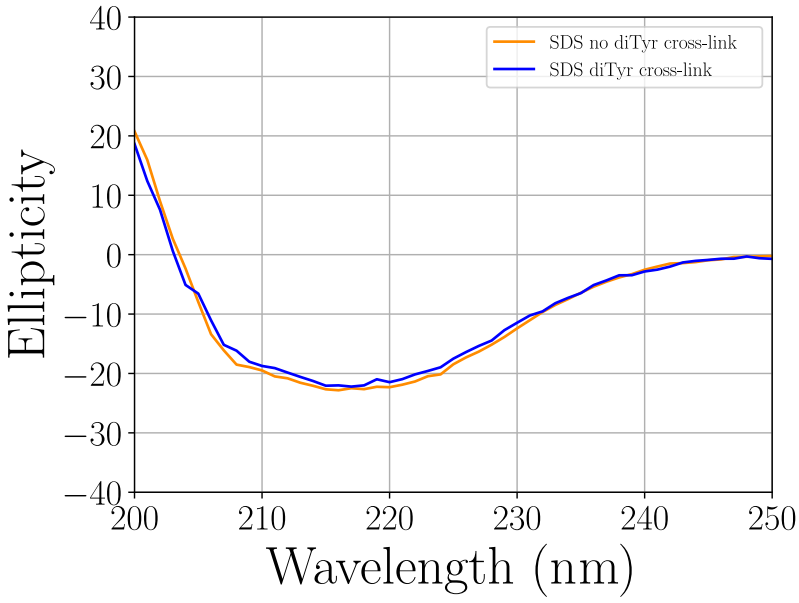

(b) Secondary structure of SDS samples before and after diTyr cross-link.

Figure 17: Illustration of SDS size fractions with and without diTyr cross-links compared with the recorded secondary structure of both size fractions.

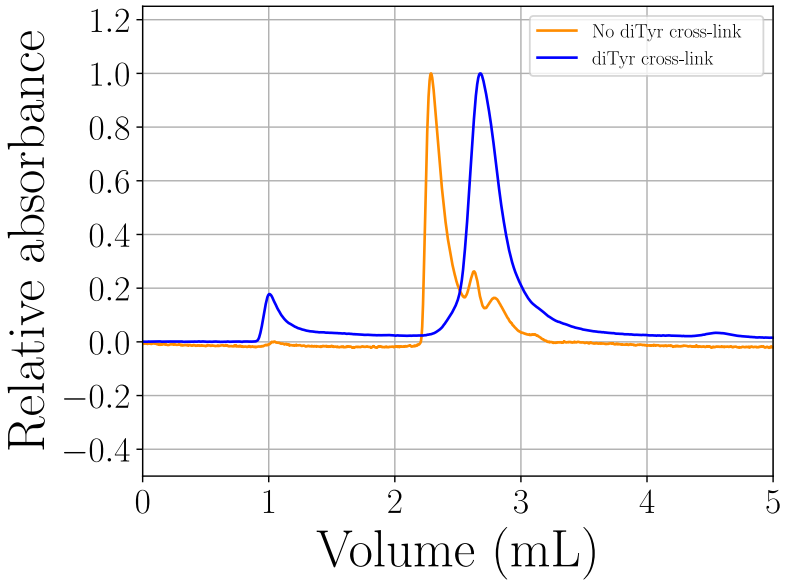

(a) Comparison between size fractions from samples, without detergent, before and after diTyr cross-link.

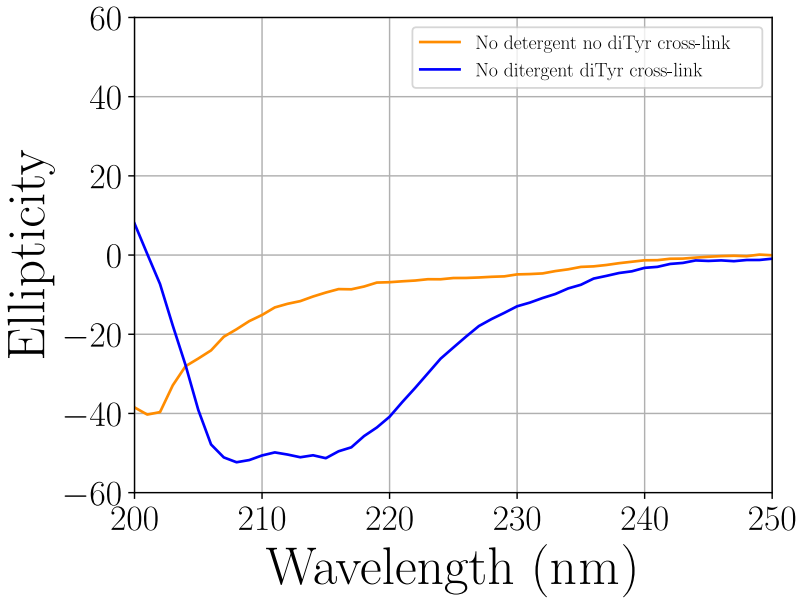

(b) Secondary structure of samples, without detergent, before and after diTyr cross-link.

Figure 18: Illustration of no-detergent size fractions with and without diTyr cross-links compared with the recorded secondary structure of both size fractions.

B Mass Spectrometry

Table 2: Mass spectrometry without diTyr

	Oligomer number							
Charges	**1**	**2**	**3**	**4**	**5**	**6**	**7**	**8**
1	4515	9030						
2	2258	4515	6773	9030				
3	1505	3010	4515	6020	7525			
4	1129	2258	3386	4515	5644	6773		
5	903	1806	2709	3612	4515	5418	6321	
6	753	1505	2258	3010	3763	4515	5268	6020
7		1290	1935	2580	3225	3870	4515	5160
8		1129	1693	2258	2822	3386	3951	4515
9			1505	2007	2508	3010	3512	4013
10			1355	1806	2258	2709	3161	3612
11				1642	2052	2463	2873	3284
12					1881	2258	2634	3010
13						2084	2431	2778
14							2258	2580

Table 3: Mass spectrometry with diTyr

	Oligomer number							
Charges	**1**	**2**	**3**	**4**	**5**	**6**	**7**	**8**
1	4515	9030						
2	2258	4515	6773	9030				
3	1505	3010	4515	6020	7525			
4	1129	2258	3386	4515	5644	6773		
5	903	1806	2709	3612	4515	5418	6321	
6	753	1505	2258	3010	3763	4515	5268	6020
7		1290	1935	2580	3225	3870	4515	5160
8		1129	1693	2258	2822	3386	3951	4515
9			1505	2007	2508	3010	3512	4013
10			1355	1806	2258	2709	3161	3612
11				1642	2052	2463	2873	3284
12					1881	2258	2634	3010
13						2084	2431	2778
14							2258	2580

C SDS Polyacrylamide Gel

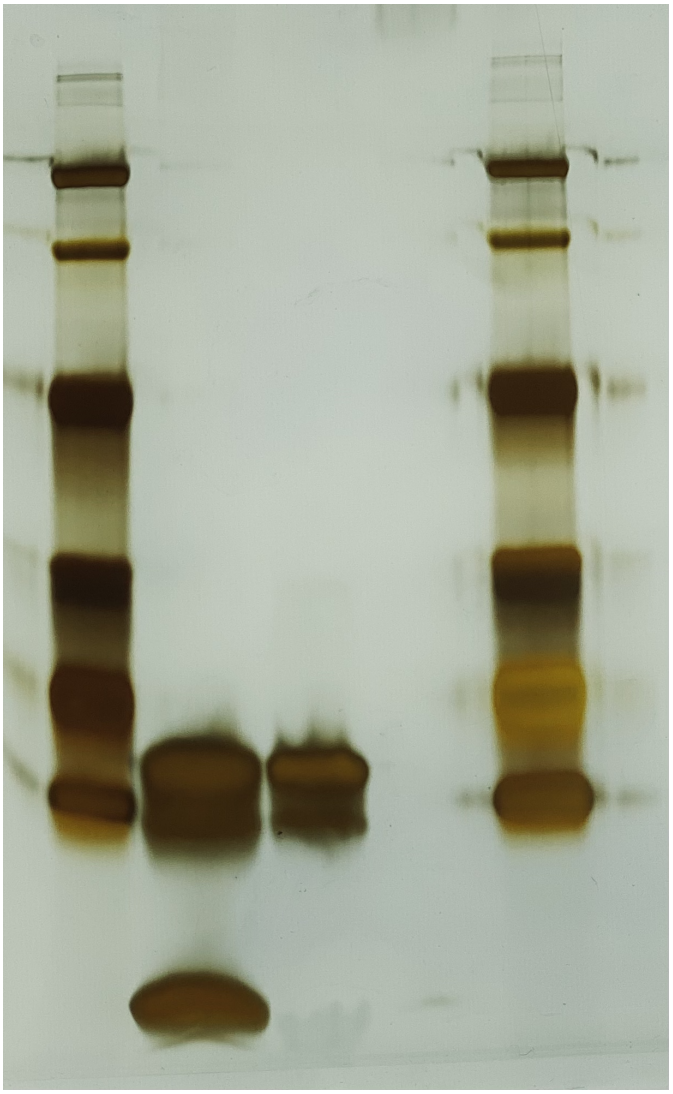

Figure 19: SDS polyacrylamide gel colored with the Pierce™ Silver Stain Kit.